COOLING CRUSTS CREATE CONCOMITANT CRYOVOLCANIC CRACKS. M. L. Rudolph[1], M. Manga[2] M. Walker[3], and A. R. Rhoden[4], [1]Department of Earth and Planetary Sciences, University of California, Davis, CA (maxrudolph@ucdavis.edu), [2]Department of Earth and Planetary Science, University of California, Berkeley, CA [3]Planetary Science Institute, Tucson, AZ, [4]Southwest Research Institute, Boulder, CO

Overview: The orbital and internal evolution of the ice-covered ocean worlds orbiting Jupiter and Saturn are coupled, leading to time-varying thicknesses of their ice shells. As the ice thickens and thins, thermal stresses in the ice shell and pressure in the underlying ocean will change, promoting and hindering fracturing of the ice shell. We solve the coupled thermo-visco-elastic equations to compute the stresses in a spherically symmetric ice shell coupled to the pressure evolution in the ocean. We identify when and at what depth cracks initiate and whether they can penetrate the entire thickness of the icy shells of Europa and Enceladus. For an ice tensile strength of 1-3 MPa, cracks do not penetrate the ice shell of Europa. On Enceladus, a plausible combination of time-averaged ice shell thickness less than 12 km and variations in tidal dissipation of more than 15% over each 100 Myr eccentricity cycles enable cracks to cross the ice shell and permit eruptions from the ocean.

Background: Cryovolcanism is actively occurring on Saturn's moon Enceladus [1], may be occurring on Europa over multi-decadal timescales [2,3,4] and may occur on other icy bodies [5]. The eruption of mixtures of ice, gas, and water requires the existence of a pathway through which material can ascend. Eruptions can be driven by a combination of buoyancy of the cryovolcanic mixture, overpressure in the subsurface ocean or reservoir [6,7], by the exsolution and expansion of dissolved gases [8] or by decompression boiling [9,10].

When a planetary ice shell thickens or thins due to melting or solidification at the ocean-ice interface, two phenomena occur simultaneously that can promote cryovolcanism. First, the volume change as liquid water solidifies increases pressure within the subsurface ocean. In turn, this pushes the ice shell outwards, generating global tensile stresses. Second, as the ice shell thickness evolves, the changing temperature gradient generates thermal stresses within the ice shell. Both of these processes can generate ~MPa stresses [7,11] - an order of magnitude larger than stresses associated with tidal deformations - and large enough to overcome the tensile strength of intact water ice.

Methods: We model the temperature and stresses in a planetary ice shell in 1D, assuming spherical symmetry. Our model includes time-dependent conductive heat transport and accounts for the release of latent heat during melting/solidification at the base of the ice shell. The form of the momentum equation adopted here accounts for thermal stresses, elastic stresses, and visco-plastic flow. The temperature and momentum equations are coupled through thermal expansion/contraction and through the pressurization of the subsurface ocean. We account for the strong temperature-dependence of ice viscosity which gives rise to viscosity variations of ~15 orders of magnitude between the ocean-ice interface and the surface. We incorporate a model for the tensile failure of ice and for the upward- and downward propagation of tensile cracks based on a parameterization of the results of boundary element calculations that used linear elastic fracture mechanics [12,13].

In order to quantify the effect of time-varying tidal dissipation, we introduce a sinusoidal variation in internal heating, implemented as an excess heat flux at the base of the ice shell. Motivated by models of orbital evolution in the Saturnian and Jovian systems, we consider variations in dissipation with a 100 Myr period [14,15]. The models span a range of equilibrium time-averaged ice shell thicknesses of 2-20 km and perturbations to the basal heat flux of 10-80%.

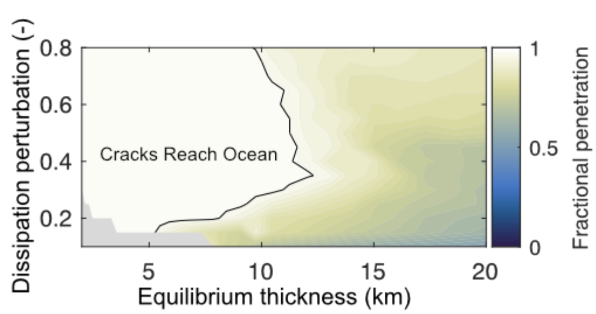

Figure 1: Fractional penetration of cracks on Enceladus. The region enclosed by the black contour indicates conditions under which cracks can connect the subsurface ocean to the surface. Models in the grey region (bottom left) do not achieve stresses large enough to create cracks.

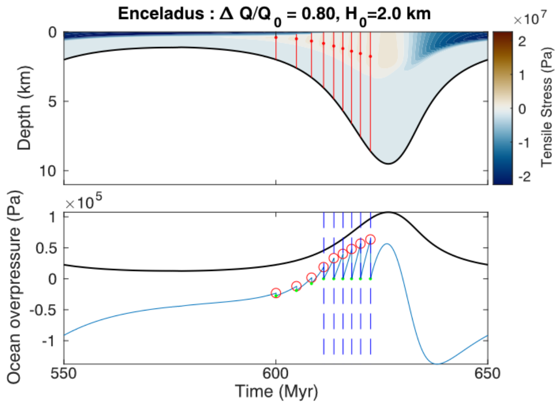

Figure 2: (top) Evolution of ice shell thickness (indicated by black curve) and tensile stresses (colors, tension positive) under Enceladus-like conditions. Here, the ice shell thickness in equilibrium with the time-averaged dissipation is 2 km and the amplitude of the time-variation in tidal dissipation is 80% of the time averaged value. The red dots indicate the location at which tensile stresses first exceed the tensile strength of ice during each cracking event (red vertical lines). (bottom) Ocean overpressure (blue curve) increases during periods of ice shell thickening and decreases during periods of ice shell thinning. The overpressure at the beginning and end of each cracking event is indicated with red and green symbols. Cracks that reach the subsurface ocean are indicated by blue vertical dashed lines. The ocean overpressure is always less than the critical overpressure necessary to extrude liquid water onto the surface, indicated by the black curve.

Results and Discussion: Cracks are not expected to reach a subsurface ocean on Europa but are possible on Enceladus for time-averaged ice shell thicknesses < 12 km and heat flux perturbation amplitudes greater than 15% of the long-term heat flow (Figure 1). We view these conditions as entirely plausible for Enceladus.

During each 100 Myr eccentricity cycle, cracks initiate below the surface during the thickening phase. Failure occurs below the surface because thermal stresses generate compressive stresses near the surface, counteracting the tensile stresses generated by ocean pressurization. Within the warmer, viscous ice, elastic stresses are not supported on the 100 Myr timescale associated with orbital evolution. If the ice is sufficiently thin (Figure1), tensile cracks can reach the subsurface ocean. In successive cracking events, failure begins at increasing depth as the thickness of the elastic ice increases (Figure 2).

We find that the ocean pressure is never large enough to overcome the buoyancy barrier necessary to extrude liquid water onto the surface of Enceladus. This result contrasts with [7], who considered much thicker ice shells which led to large enough ocean overpressure to extrude water. The models shown in the present work differ in a couple of key regards. First, they include thermal stresses, which hinder eruptions. Second, the fraction of the ice shell that supports elastic stresses is determined by solving a time-dependent heat transport equation rather than an assumed constant fraction of the ice shell thickness or constant thickness.

Although our results do not favor extrusive cryovolcanism, they do strongly support the idea of a plume sustained by the decompression boiling mechanism [9,10]. Once a crack connects the ocean to space, we expect that tidal dissipation within the crack could catalyze conduit creation, leading to sustained cryovolcanism [16].

Acknowledgments: MM, MW, and ARR acknowledge support from NASA.

References: [1] Porco, C. C. et al. (2006) *Science,* 311(5), 1393–1401. [2] Roth, L. et al. (2013) *Science,* 343(6167) 171-174. [3] Paganini, L. (2020) *Nat. Astron.,* 4(3), 266-272. [4] Jia, X. et al. (2018) *Nat. Astron.,* 2(6), 459-464. [5] Geissler (2015) *Encyc. Volc. 763-776.* [6] Fagents, S. A. (2003) *J. Geophys. Res.* 08(E12), 5139. [7] Manga, M. and Wang, C.-Y. (2007) *J. Geophys. Res.,* 34, L07202. [8] Crawford, G. D. and Stevenson, D. J. (1988) *Icarus,* 73(1), 66-79. [9] Ingersoll, A. P. and Nakajima, M. (2016) *Icarus,* 272, 319-326. [10] Nakajima, M. and Ingersoll, A. P. (2016) *Icarus* 272, 309-318. [11] Nimmo, F. (2004) *J. Geophys. Res.,* 109, E12001. [12] Rudolph, M. L. and Manga, M. (2009). *Icarus*, 199, 536-541. [13] Hemingway, D. L. et al. (2020) *Nat. Astron.,* 4(3), 234-239. [14] Hussman, H. and Spohn, T. (2004) *Icarus*, 171(2), 391-410. [15] Shoji et al., (2014) *Icarus*, 235, 75-85. [16] Kite, E. S. and Rubin, A. M. (2016) *PNAS*, 113(15) 3972-3975.